Heliyon 6 (2020) e05104

Contents lists available at ScienceDirect

Heliyon

journal homepage: www.cell.com/heliyon

Research article

Extraction, optical properties, and aging studies of natural pigments of various flower plants

S.M. Amir-Al Zumahi [a,b], Nourin Arobi [a,b], Hatem Taha [c], Md Kamal Hossain [a], Humayun Kabir [a,d], Rummana Matin [e], M.S. Bashar [e], Farid Ahmed [a], Md Abul Hossain [a], M. Mahbubur Rahman [a,f,*]

[a] Department of Physics, Jahangirnagar University, Savar, Dhaka 1342, Bangladesh
[b] Bangladesh Atomic Energy Commission, Dhaka 1207, Bangladesh
[c] Department of Physics, College of Education for Pure Science, Ibn Al-Haitham, University of Baghdad, 10071, Baghdad, Iraq
[d] School of Engineering, RMIT University, Bundoora, Victoria 3083, Australia
[e] Institute of Fuel Research and Development (IFRD), Bangladesh Council of Scientific and Industrial Research (BCSIR), Dhaka 1205, Bangladesh
[f] Discipline of Chemistry and Physics, College of Science, Health, Engineering and Education, Murdoch University, Perth, WA 6150, Australia

ARTICLE INFO

Keywords:
Materials science
Natural dyes
Pigment
Absorption spectra
Dye extraction methods
Ageing effect

ABSTRACT

In this paper, we reported the extraction process of five different flowering plants utilizing different dye extraction methods and solvents (ethanol and water) to choose the best dye removal process. The FTIR spectra revealed the presence of several clear functional groups for all five natural dyes. The analytical studies such as UV spectroscopy, column chromatography, and vacuum evaporation were performed to isolate the dyes from their solutions. The UV-Vis studies on the pigments of flower extracts indicated broad absorption peaks in the visible region including clear bandgaps. Among the studied pigments, *Alternanthera ficoidea* showed the lowest direct bandgap of 1.69 eV and an Urbach energy value of 6.33 meV. The dye extraction yield rate improvement was extended from 11.7 to 24.7% (water solvent) and 11.3–32.4% (ethanol solvent). Throughout the studies, it was observed that ethanol produced a better extraction for organic dyes than water as a solvent. Aging studies revealed that all the dyes at the room temperature showed better stability with minor changes in the observed optical parameters in oxygen-rich conditions; however, these parameters have shown significant variations at a 60 °C temperature.

1. Introduction

The dyes have been a vital factor in the culture of people throughout the world. Dyes are not only used in a way to beautify an item but also to demonstrate the culture of different places and provide shreds of evidence on the disparities from ancient civilizations. Without chemical processing, dyes acquired from nature are known as natural dyes. Natural dyes come from different sources such as plants, minerals, insects, and/or animals. They are non-toxic and, in most cases, non-allergic. Natural dyes are an essential part of human life, environmentally friendly, harmless during use, also maintains the ecological balance [1, 2, 3]. The invention of synthetic colorants in the 19th Century reduced the use of natural dyes. Synthetic dyes are regarded as superior terms of aesthetic appeal and scope of coloring, strength, and cost-efficiency. In the 20th Century, careful studies of synthetic dyes were carried out in conservation and restoration. Furthermore, investigating conventional dyeing techniques have been a significant aspect of social history, as seen from earlier reports [4, 5, 6]. Recent studies showed that over 100,000 types of commercial dyes exist, and more than 7 $\times$ 10^5 tons per season have been produced annually [7, 8].

The innovation of principal synthetic dye by Perkin [9, 10, 11] has changed the situation. Consequently, the production of synthetic dyes increased at great speed as they found favor as alternatives to natural dyes in foods [12, 13, 14], non-linear optical movements [15, 16], cosmetics [17, 18, 19], and material commercial ventures [20] because of straightforwardness in dyeing, and the cost factor. Considering the energy saving and ecological security, shading of materials with natural dyes has been given more significant consideration by experts and manufacturers. Researchers working in this area are now taking steps to improve the pigment extractions from plant materials [21, 22, 23, 24, 25], such as petals, leaves, bark, and seed, to enhance the percentage of yield. Specific techniques such as magnetic stirring, ultrasound-assisted

* Corresponding author.
E-mail address: m.rahman@juniv.edu (M.M. Rahman).

https://doi.org/10.1016/j.heliyon.2020.e05104
Received 4 July 2020; Received in revised form 15 August 2020; Accepted 25 September 2020

extraction, subcritical water extraction, soxhlet process, and supercritical fluid extraction are suggested to increase the dye yield [26, 27, 28, 29].

It has been reported that, natural dyes can be easily extracted from different natural plants, such as yellow marigold [30, 31, 32], pomegranate [33, 34], alpinia blepharocalyx K. schum [35, 36], grape pomace [37], henna leaves [38], mango leaves [39], butea monosperma [40], red calico leaves [41], rosella [42], and blue pea flowers [43]. These organic compounds contain hydroxyl groups, and are poorly water-soluble and usually contain various pigments, including chlorophyll, carotene, luteol, violaxanthol, phycoerythrins, and phycocyanins in the flowers, petal or plant leaves [44, 45, 46, 47]. The use of extraction enhancement and various pigment functionalities in different natural coloring processes has been a recent research topic. However, it is imperative to improve extraction techniques to identify the right strategy for various artificial dyes applications. A significant issue in improving extraction is enhancing the stability and processing to prevent the degradation of the color-fastness of colors and/or their pigments. The causes of degradation are exogenic reasons such as temperature, humidity, and air and light [48, 49, 50]. The most effective exogenic factors are oxygen and temperature. It is also known that with or without oxygen intervention, the dyes fastness and internal properties may be degraded.

Nowadays, natural dyes' aging effects at different time intervals due to exogenic factors remain attractive area research worldwide. It is crucial to use the proper solvent for natural dye extraction methods. Distilled water and ethanol found to perform the best as polar solvents for organic dye extractions due to their higher solubility and less polarity. For that reason, we choose these solvents to make a fair comparison to our experimental results. Among the five organic dyes reported in this paper, two of them (*pereskia bleo* and *alternanthera ficoidea*) new, and no work has been found in the literature. The activation and inactivation of pigments with absorption under two different solvents were investigated. These pigments were characterized using aging studies at two different temperatures in the compositional and optical analysis.

Given these factors, this paper is concerned with analyzing and reporting the extracted dye pigments' activity and inactivity in two different solvents (water and ethanol). Five natural plants have been cultivated, and investigated to assist with the recognition and identification of various pigments which are present in the extracts of natural

Figure 1. Raw materials of extracted dyes used in present research (also in Table 1): (a) *portulaca grandiflora* (time flower) (b) *rosa ards rovar* (red rose) (c) *celosia argentea var. cristia* (plumbed cockscomb) (d) *pereskia bleo* (desert rose) (e) *alternanthera ficoidea* (border plant).

Table 1. Description of the raw materials (natural dyes).

English name	Botanical name	Plant family	Used parts	Color of used parts
(a) Time Flower	*Portulaca grandiflora*	Portulacaceae	Petals	Deep pink
(b) Red rose	*Rosa ards rovar*	Rosacea	Petals	Red
(c) Plumbed cockscomb	*Celosia argentea ver. Cristia*	Amaranthaceae	Comb of roster	Light red
(d) Desert rose	*Pereskia bleo*	Cactaceae	Petals	Orange
(e) Border plant	*Alternanthera ficoidea*	Amaranthaceae	Leaves	Light pink

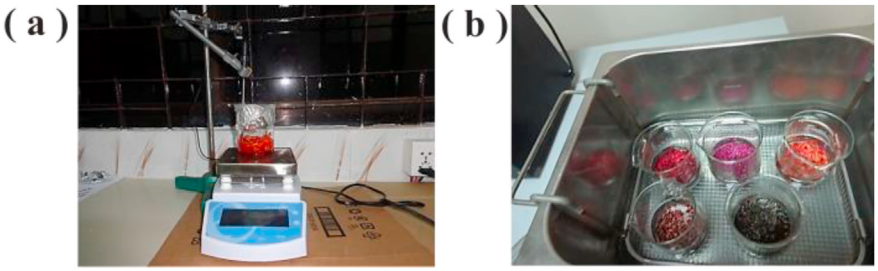

Figure 2. Extraction process of different natural dyes with water and/or ethanol solvent for (a) magnetic stirring and (b) ultrasound assisted extraction from 1g in 50ml solvent at 45 °C for 1h.

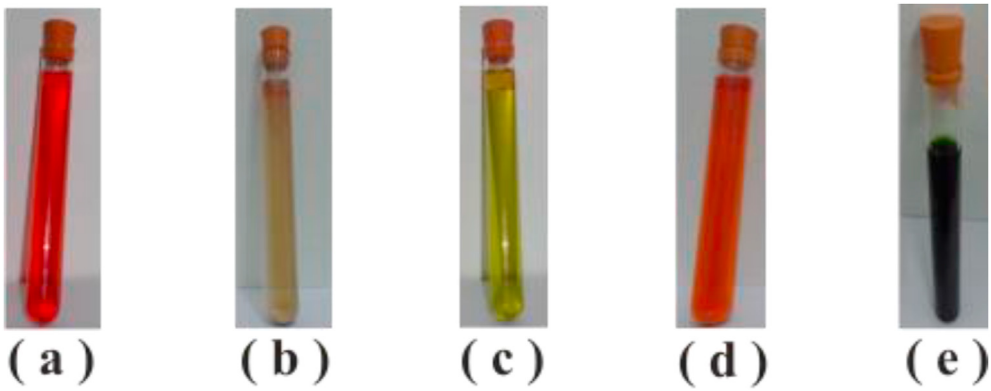

Figure 3. Visual appearance of extracted dyes from natural plants of (a) *portulaca grandiflora* (deep pink) (b) *rosa ards rovar* (light gray) (c) *Celosia argentea var. cristia* (light green) (d) *Pereskia bleo* (orange) (e) *Alternanthera ficoidea* (bluish green).

dyes with ethanol and water solvent; and to develop them ecologically and economically with regards to their percentage of yields, improvement of extraction, structural, and optical properties. In the water solvent case, the aging studies (in 60 days interval) of the extracted pigments have been conducted *via* FTIR and UV-Vis spectroscopy.

2. Experimental

2.1. Materials and methods

Portulaca grandiflora, Celosia argentea var. cristia, Rosa ards rovar, Pereskia bleo flowers petal and *Alternanthera ficoidea* plants leave have been used for as the source of extracting dyes. All these five plants are incredibly available at the green campus of Jahangirnagar University. The pictures of these flower plants are shown in Figure 1. A brief description of them has been outlined in Table 1.

A magnetic stirring (MS300 Hot Plate Magnetic Stirrer, Model MS300), and an ultrasonic extraction machine (Dispositivo ULTRASUONI Bandelin Sonorex DK 102P Digital 10P) were used to extract the natural dyes. The magnetic stirrer has a stirring volume of 0–2000 ml, stirring speed 0–1250 rpm, and heating temperature 0–300 °C. Heidolph solvent evaporation by Germany was used for vacuum evaporation (the fixed temperature at 50 °C and pressure 60 mbar with 100 rpm) to collect dry dye.

The FTIR spectra were collected using the Shimadzu IR Prestige 21. The Ultraviolet visible spectra were acquired using the GBC Cintra 2020 UV-Visible spectrometer that operated in the wavelength range of 200 nm–1100 nm for water solvent, and 400 nm–1100 nm for ethanol solvent, respectively. It has a very low divergent light and noise specifications.

2.2. Dye extraction process

Natural dye bearing *Portulaca grandiflora, Celosia argentea var. christie, Rosa ards rovar, Pereskia bleo* and *Alternanthera ficoidea* flower samples were isolated into individual petals. The samples were carefully washed using distilled water. Collected petal samples with an average size of 0.5 cm were used to dry at room temperature. 1g of dry petals, from each sample, were taken and 50 ml water or ethanol solvent was introduced in a glass beaker to immerse the petals into the solvent fully. Figure 2 indicates the magnetic and ultrasound-assisted extraction process for two different solvents: water and ethanol.

The ratio of the natural dye and water/ethanol solvent was 1:50. The operating condition for the magnetic stirring and ultrasonic extraction (with medium sonic power 10 × 10%) of natural dyes from *Portulaca grandiflora, Rosa ards rovar, Celosia argentea var. cristia, Pereskia bleo, and Alternanthera ficoidea* were optimized at 45 °C for 60 min. According to the ethanol solvent's volatile properties during extraction, aluminum foil has been used on the top of the beaker to minimize evaporation. The extracted liquid dyes have been shown in Figure 3. Extracted pigments were taken for further purification by column chromatography.

2.3. Aging effects

The aging effects are the degradations of natural dyes in the presence of oxygen and ozone which is facilitated by the incident light. After extracting the natural dyes, it is important to know the aging effects in order to realize the nature of color fading and/or intermolecular bond stability. The aging effects of the extracted dyes have been investigated *via* analyzing the absorption and FTIR spectra with water solvent at room temperature and at 60 °C in a 60 day time interval.

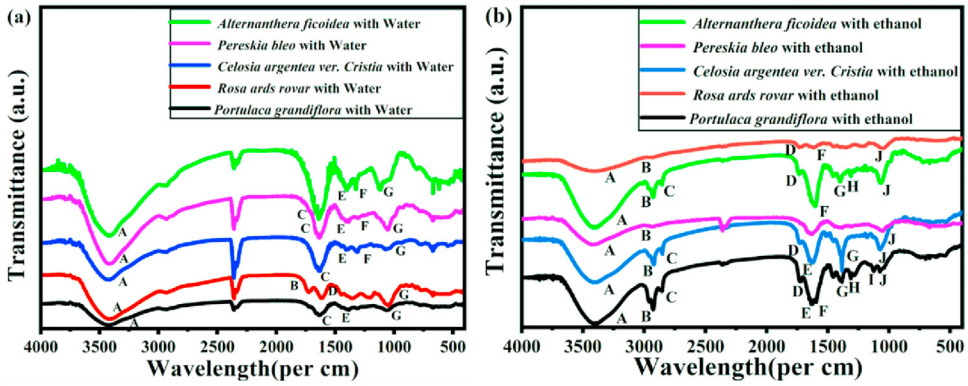

Figure 4. Fourier transform infrared spectroscopy of as extracted natural dyes at room temperature with (a) water and (b) ethanol solvent using ultrasonic extraction.

Table 2. Structural composition of natural dyes according to their different bonds of water and ethanol solvent using ultrasonic extraction process as required from IR spectroscopy.

Peak	Dye extraction with water solvent		Dye extraction with ethanol solvent	
	Peak value (cm^{-1})	Description	Peak value (cm^{-1})	Description
A	3422	stretching of ν O–H (alcohol)	3400	stretching ν O–H (alcohol)
B	1722	Stretching Carbonyl ν C=O (Ester)	2934	Aromatic ν C–H
C	1689	Stretching Olefinic ν C=C	2851	Stretching Aliphatic ν C–H
D	1611	stretching Aromatic ν C=C	1731	Stretching Carbonyl ν C=O (Ester)
E	1400	bending $–CH_3$ group	1635	Stretching Olefinic ν C=C
F	1311	bending $–CH_2$ group	1614	aromatic ν C=C
G	1049	stretching ν C–O	1387	bending $–CH_3$ group
H	-	-	1314	bending $–CH_2$ group
I	-	-	1123	stretching ν C–C
J	-	-	1065	stretching ν C–O

3. Result and discussions

3.1. Fourier transform infrared (FTIR) spectroscopy

The composition of natural dyes has been affirmed using FTIR spectroscopy, has been shown in Figure 4. A brief analysis of the FTIR spectra of five sample has been displayed in Table 2. Since various peaks obtained in FTIR studies of individual samples are approximately very similar, we have collectively expressed them employing capital letters in Table 2 (in two different sections: one for water and the other for ethanol). The main difference between Figure 4(a) and (b) is that in spectrum 4(a) the stretching band for aromatic ν C–H, and aliphatic ν C–H is not clear, but in spectrum 4(b), a sharp peak is seen at B (2934 cm^{-1}) and C (2851 cm^{-1}). Except for *Rosa ards rovar* and *Pereskia bleo* in Figure 4(b), all dyes with ethanol solvent shows sharp B and C peaks due to the aromatic ν C–H and aliphatic ν C–H stretching frequencies, respectively. In Figure 4(a), the band B at 1722 cm^{-1} is due to Ester Carbonyl (ν C=O) stretching frequency while in Figure 4(b) the stretching band for Ester Carbonyl appears at D (1731 cm^{-1}). It is also seen that in Figure 4(a), another band C detected at 1689 cm^{-1} is for Olefinic ν C=C stretching while in spectrum 4(b), the same peak appears at E (1635 cm^{-1}). In Figure 4(a), another band D found at 1611 cm^{-1} is due to the stretching frequency of aromatic ν C=C is not sharp, but in spectrum 4(b), the aromatic ν C=C band is sharp at F (1614 cm^{-1}). In the wavenumber range of 1000–1500 cm^{-1}, considerable isotropic properties (see Figure 4(a)) have been seen in *Portulaca grandiflora, Rosa ards rovar, Celosia argentea var. cristia,* and *Pereskia bleo* with low bending groups such as $–CH_2$, and $–CH_3$. On the other hand, *Alternanthera ficoidea* has shown anisotropic properties. Further investigations revealed that all the samples within the same region demonstrated the isotropic behavior with higher bending groups $–CH_2$, and $–CH_3$ (see Figure 4(b)). Our results are in good agreement with earlier reports [51, 52, 53, 54].

3.2. UV-Vis spectroscopy

Figure 5(a) and (b) show the UV visible spectra of five dye samples with water, and ethanol solvent, respectively. The obtained absorption spectrum was very sharp for all the extracted dyes at different wavelengths, varying their intensity levels. Figure 5(a) shows that a sharp peak of *Portulaca grandiflora* dye solution is at the wavelength of 539 nm for water solvent. The ethanol dye solution revealed a major improvement in the absorption spectrum by introducing a new peak at 498 nm with a bathochromic shift of nearly 41 nm from the spectrum of water solvent extraction (see Figure 5(b)). The *Rosa ards rovar* spectrum (red line) has shown an isotopic behavior for both solvents. Figure 5 also indicates that the *Pereskia bleo* illustrated some clear peaks at 452 nm, 478 nm, and 545 nm (in the visible range for water solvent). Still, ethanol-based extraction displayed a sharp peak at 497 nm while the other peaks were disappeared. The absorbance spectra of the *Celosia argentea var. cristia* (green line) and *Alternanthera ficoidea* (blue line) dye solution in water differs from that extracted using the ethanol solvent. The *Celosia argentea var. cristia* (280 nm), and *Alternanthera ficoidea* (265 nm and 337 nm) spectra have shown a few weak peaks for water solvent. In contrast, ethanol-based spectra demonstrated very high intense peaks in 450 nm–700 nm (see Figure 5(b)). As predicted, the level of light absorption in the ethanol-based extracted pigments was considerably greater than that of the water-based extractions.

3.3. Effect of solvent on extraction

Figure 5 showed the solvent's effect on the absorption spectra of five flower pigments extracted using ethanol and water. The absorbance of *Portulaca grandiflora*, *Rosa ards rovar*, *Celosia argentea var. cristia, Pereskia bleo*, and *Alternanthera ficoidea* demonstrates a scope of wavelength recurrence between 400 nm–700 nm, which is situated in the visible range. As seen from the spectra's curves, the absorption peak value of the *Portulaca grandiflora* of ethanol solvent is 460 nm and 498 nm, which indicates the pigment γ carotene and 665 nm indicates Chlorophyll *a* from the absorption maxima Table 3. The water-based absorption peak value of *Portulaca grandi flora* is 539 nm, which indicated phycoerythrins pigment. From the figure, it is easily concluded that phycoerythrins are inactive in the ethanol-based dye solution. On the other hand γ carotene, and Chlorophyll a are active in the water-based dye solution. In *Pereskia bleo*, the Phycoerythrins (545 nm), and Violaxanthol (452 nm, and 478 nm) are active in the water solvent. In comparison, γ carotene (497 nm), and Phycocyanin (590 nm, and 614 nm) are active in the ethanol solvent. The Phycoerythrins (537 nm, 540 nm, 549nm, 578 nm, and 588 nm), Chlorophyll a (670 nm, 675 nm, and 680 nm), Phycocyanins (618 nm), β carotene (478 nm), and Chlorophyll *b* (627 nm) are active in the ethanol solvent for *Rosa ards rovar, Celosia argentea var. cristia*, and *Alternanthera ficoidea respectively* but inactive in the water-base dye solution. The dye solutions of *Rosa ards rovar, Celosia argentea var. cristia*, and *Alternanthera ficoidea have* no active pigments between 400 nm and 800 nm. The calculations of the optical bandgap utilizing UV-Vis absorbance spectra was achieved *via* Tauc relation [57]. Figure 5 (a.1 & b.1) and (a.2 & b.2) show the Tauc plots for direct and indirect bandgaps, respectively, while Table 4 represents the samples' bandgap and Urbach energy values. Based on Table 4, the remarkable observations of the direct and indirect optical bandgaps of *Portulaca grandiflora, Rosa ards rovar*, and *Pereskia bleo* have increased for the ethanol solvent. At the time that of the plumed cockscomb and border plants have dwindled. The lowest bandgap was 1.77 eV for the *Rosa ards rovar* (water-based extraction), and 1.67 eV for the *Alternanthera ficoidea* (ethanol-based extraction).

Several defect bands are developed throughout the optical absorption system as just an intermediate state within the bandgaps of the

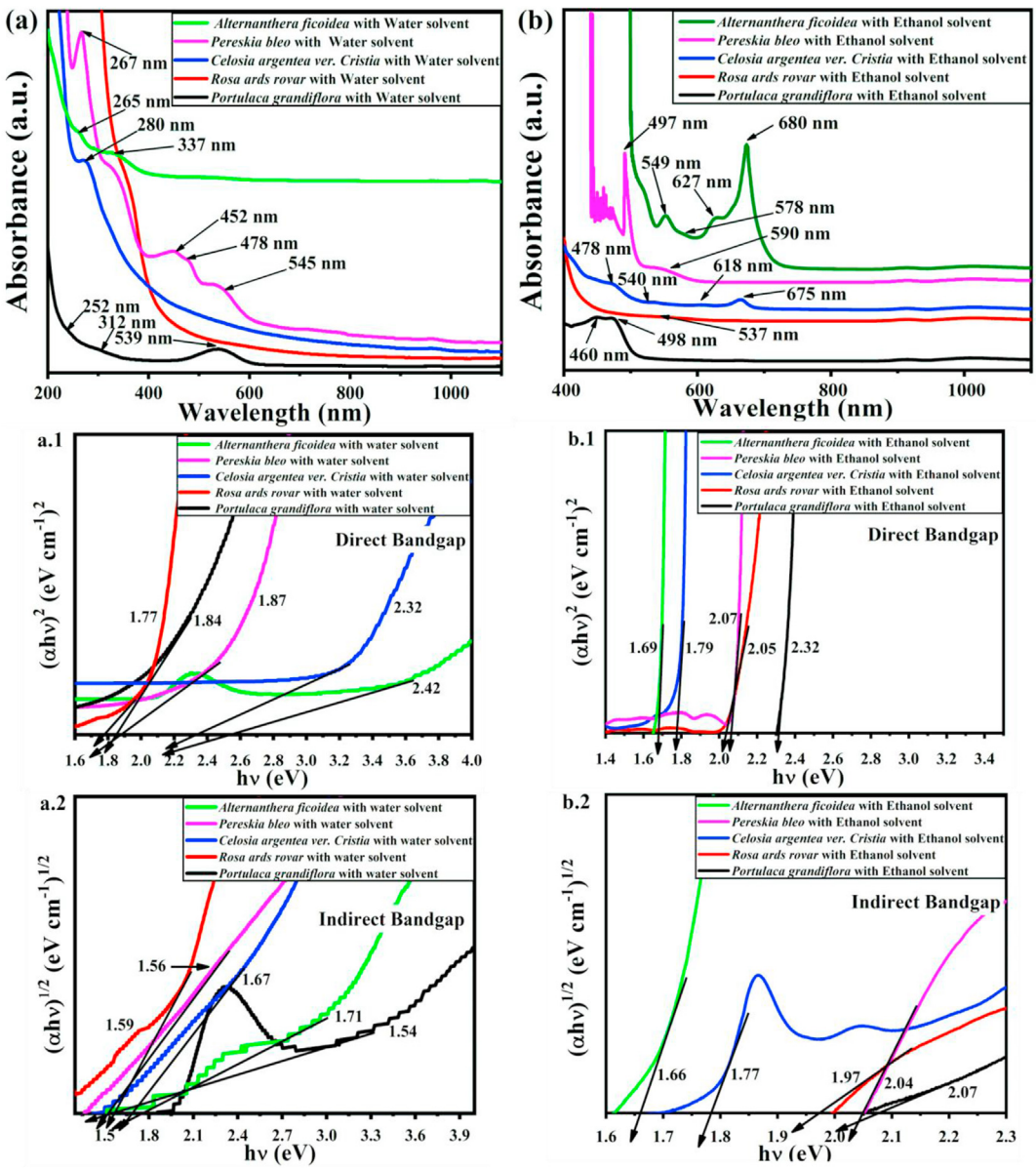

Figure 5. Optical absorption spectra of five different extracted dyes for (a) water and (b) ethanol solvent, where (a.1-b.1) and (a.2-b.2) indicates direct bandgap and indirect bandgap using Tauc relation.

Portulaca grandiflora, Celosia argentea var. cristia, Rosa ards rovar, Pereskia bleo, and *Alternanthera ficoidea*. These defect bands generate an energy tail that extends from both the bottom of the conduction bands and top of the valence bands to the deep of the bandgap [58, 59]. This energy correlated defect tail is termed as the Urbach energy provided by Eq. (1) [60],

$$\alpha = \alpha_0 \, e^{\frac{h\theta}{E_U}} \tag{1}$$

Where α_o, α and E_U denote the constant, absorption coefficients, and Urbach energy (energy of the band tail), respectively. Taking natural log on both sides of the equation, one obtains a straight line equation such as given by Eq. (2),

Table 3. Absorption maxima for natural dyes (different pigments) comparison with other research work according to their wavelength (nm).

Pigment	Reported wavelength (nm) [55, 56]	Obtaining wavelength (nm)	Occurrence
Chlorophyll *a*	430, 670	675,670,665,680	All green plants
Chlorophyll *b*	455, 640	627	Higher plants, green algae
α-carotene	420,440,470	446	Leaves, some algae
β-carotene	425,450,480	484,478	Some plants
γ-carotene	440,460,495	460,498,497	Some plants
Luteol	425,445,475	474	Green leaves, red and brown algae
Violaxanthol	425,450,475	478	Some leaves
Phycoerythrins	490,546,576	539,540,588,549,578	Red and blue-green algae
Phycocyanins	618	618,614,590	Red and blue-green algae

Table 4. Calculated bandgap (direct and indirect) and Urbach energy of natural dyes for the extraction of water and ethanol solvent by ultrasound-assisted extraction.

Dye solution	Band gap (eV)				Urbach energy (meV)	
	Water solvent		Ethanol solvent		Water solvent	Ethanol solvent
	Direct	Indirect	Direct	Indirect		
Portulaca grandiflora	1.84	1.54	2.32	2.07	8.03	13.94
Rosa ards rover	1.77	1.59	2.05	1.97	3.07	3.59
Celosia argentea ver. Cristia	2.32	1.67	1.79	1.77	1.24	3.48
Pereskia bleo	1.87	1.56	2.07	2.04	2.42	8.06
Alternanthera ficoidea	2.42	1.71	1.69	1.66	2.32	6.33

$$ln\alpha = ln\alpha_0 + \frac{h\vartheta}{E_U} \tag{2}$$

Plotting lnα versus $h\nu$, it is possible to obtain the Urbach energy from the straight line's slope. The Urbach energy (both for water and ethanol solvent) calculations using the variation of lnα curves with respect to the incident photon energies have been shown in Figure 6, and the measured values for all specimens are displayed in Table 4.

Urbach energy of the ethanol-based extraction is found to increase in comparison with the water-based extract. Further investigation also indicated that Urbach energy values and bandgaps are show opposite behavior for the ethanol-based and water-based extractions *i.e.*, bandgaps are greater in water than Urbach energy values and vice versa [61]. The higher estimated Urbach energies of *Portulaca grandiflora* for ethanol solvent is 13.94 meV while *Celosia argentea ver. Cristia* shows the lowest for water (see Table 4). Urbach energy is related to the structural disorder mechanism of a system [62]. Higher Urbach energy means more disorders induced by insufficient crystalline or amorphous solid structures [63]. Among both solvents, the water-based samples have the minimum Urbach energy suggesting less crystal disturbance, supporting the less functional shift in the water-based FTIR spectroscopy (see Figure 4a). The reported variations could be related to the change in the internal fields related to the chemical group interaction or fewer ability to transform weak bonds into defects.

The optical transmittance spectra of five organic dyes have been shown in Figure 7. The transmittance of natural dyes falls off rapidly around the UV-Vis boundary, and the transmittance is negligible in UV-regions for the water-based extraction (Figure 7(a)). However, the ethanol-based extracted natural dyes fall off in the visible regions. All the dye samples showed anisotropic properties except *Portulaca grandiflora* and *Rosa Ards rovar* in Figure 7(b). The refractive index is one of the fundamental parameters to determine the optical properties of a sample. Refractive index detection is commonly used for the analysis of dyes or compounds that has low absorption ranges. The refractive index has been computed utilizing Swanepoel's method. As per Swanepoel's formula, the refractive index (n), at a given wavelength, can be calculated using the following Eq. (3) [64],

$$n = \left[N_1 + \left(N_1^2 - s^2\right)^{\frac{1}{2}}\right]^{\frac{1}{2}} \tag{3}$$

Where, $N_1 = 2s\frac{T_M - T_m}{T_M T_m} + \frac{s^2+1}{2}$

Here T_M and T_m indicate the upper envelop transmittance and the lower envelop transmittance respectively, at a specific wavelength λ. $s = 1.51$, depends on the wavelength and may be calculated using the transmittance spectra.

Figures 8(a) and (b) displayed the variations of the refractive index for natural dyes as a function of incident photon wavelength (nm) for water and ethanol, respectively. All the extracted pigments showed nearly equal refractive index value (1.51) for both solvent, but only *Alternanthera ficoidea* and *Pereskia bleo* reach the maximum

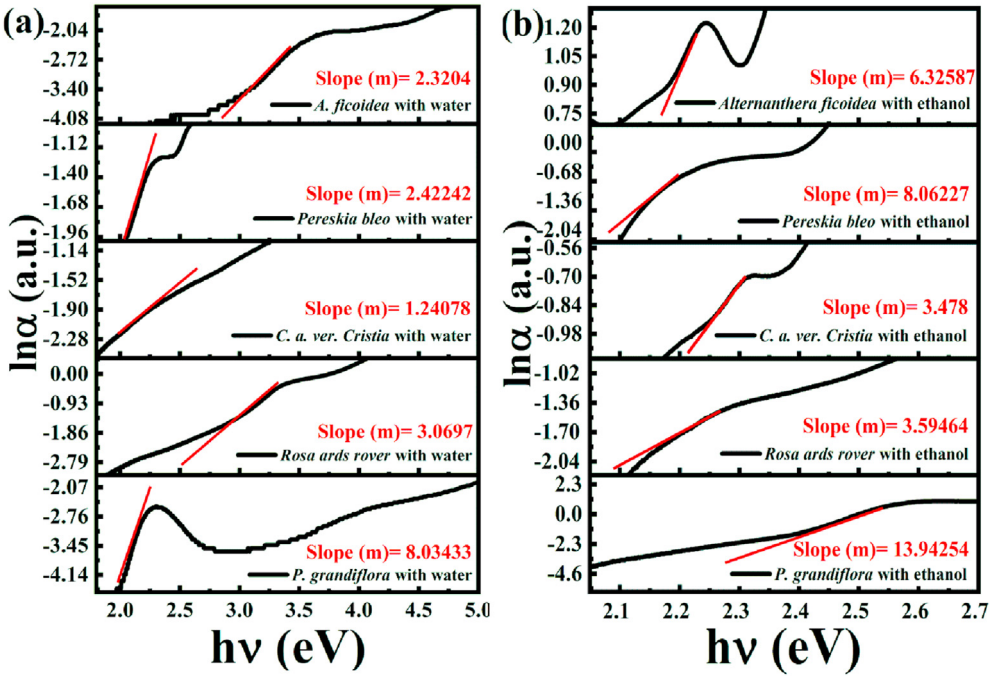

Figure 6. Urbach energy calculation in accordance with graphical slope of photon energy versus lnα for extracted dyes at room temperature with (a) water and (b) ethanol solvent.

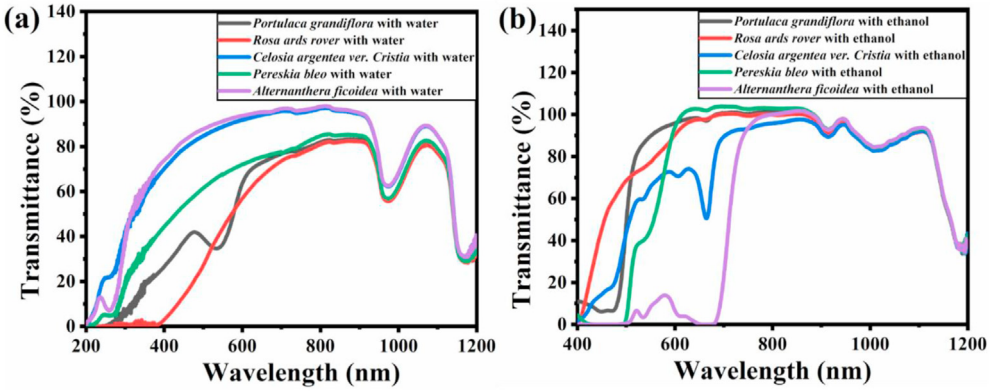

Figure 7. Transmittance spectra of natural dyes as a function of wavelength (nm) at room temperature with (a) water solvent from 200-1200 nm and (b) ethanol solvent from 400-1200 nm by ultrasonic extraction process.

values of 56 and 60 for ethanol solvent. The higher refractive index means slower the light travels which causes a correspondingly increased change in the light's direction within the dyes. Consequently, within the dyes, the light can bend more, thereby allowing the dyes profile to be lower [65, 66]. This high refractive index may occur due to different bonds of dyes, low absorption, and/or oxygen vacancies [67]. The non-zero refractive index components of all the dyes revealed the highest value for photon energy at the visible regions. Significant isotropic behavior has been seen in the wavelength range of 550 nm–800 nm whereas 400–550 nm showed divergences in all the solvents dyes. High refractive indices at low wavelengths are due to the effect of the fundamental absorption below 350 nm [68, 69]. In the water solvent, all dyes show refractive indices in the range of 1.50–1.95 while ethanol solvent up to 60.

3.4. Gravimetric analysis

After the vacuum evaporation process, the extracted dye solutions were measured very carefully. The percentage of yields and % improvement for ultrasonic have been measured using the following Eqs. (4) and (5) [32, 70],

$$\text{Percentage of yield} = \frac{\text{obtained natural dyes (g)}}{\text{raw material of natural dyes (g)}} \times 100\ \% \tag{4}$$

$$\%\text{improvementduetoultrasound} = \frac{\%yieldfrom(Ultrasound - Magneticstirring)}{\%yieldofmagneticstirring} \times 100\% \tag{5}$$

The percentage of yields and % improvement for ultrasonic of acquired natural dyes have been given in Table 5. Based on the results presented in Table 5, we see that each pigment (either ethanol or water extracted) exhibited a significant contrast for those extracted ingredients. For this reason, the extraction solvent choice is exceptionally imperative. The yield of the specimens using magnetic stirring and/or ultrasound-assisted extraction exhibited a lower yield of percentage of dye (0.73–4.01% for the water-based extraction) and (1.08–6.79% for the ethanol-based extraction). It has been also found that the colorant

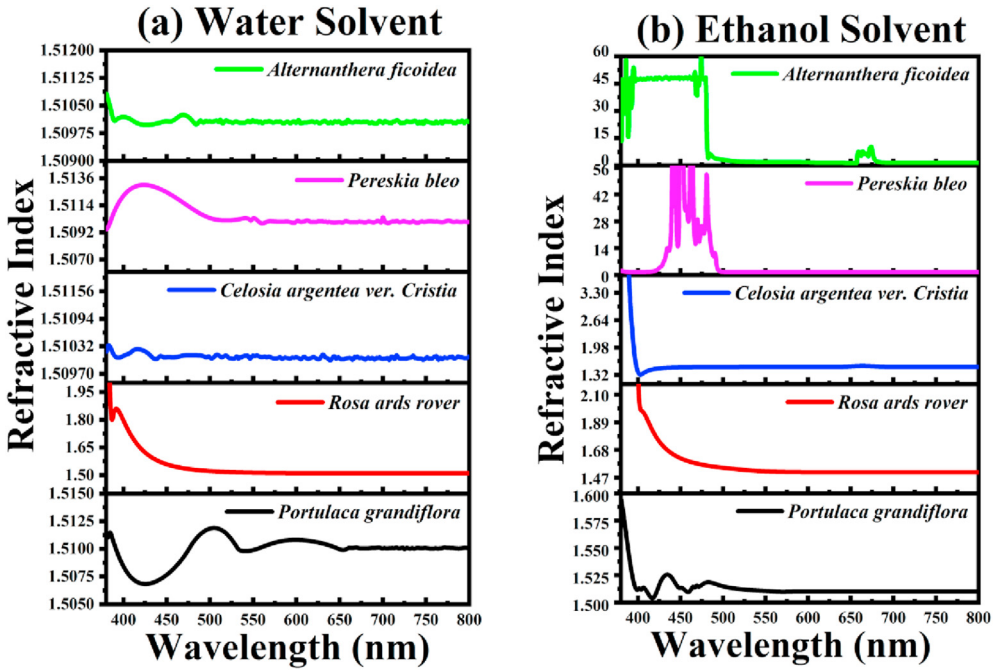

Figure 8. The variation of refractive index against wavelength (nm) of five different natural dyes with (a) water and (b) ethanol solvent for ultrasound assisted extraction process.

Table 5. Percentages of yields for dyes yielding materials and their percentage improvement for magnetic stirring and ultrasonic extraction process with ethanol and water solvent.

Sample	Raw materials weight (g)	Amount of solution (ml)	Obtained Weight (g)				Percentage of Yields (%)				% Improvement for ultrasonic	
			Extraction by magnetic stirring		Ultrasonic extraction		Extraction by magnetic stirring		Ultrasonic extraction			
			Water solvent	Ethanol solvent	Water solvent	Ethanol Solvent	Water solvent	Ethanol solvent	Water solvent	Ethanol Solvent	Water solvent	Ethanol solvent
Portulaca grandiflora	1	50	0.0073	0.0128	0.0091	0.0165	0.73	1.28	0.91	1.65	24.66	28.91
Rosa ards rover	1	50	0.0359	0.0661	0.0401	0.0679	3.59	6.61	4.01	6.79	11.7	11.3
Celosia argentea ver. Cristia	1	50	0.0067	0.0108	0.0083	0.0143	0.67	1.08	0.83	1.43	23.88	32.4
Pereskia bleo	1	50	0.0119	0.0287	0.0135	0.033	1.19	2.87	1.35	3.3	13.45	15
Alternanthera ficoidea	1	50	0.011	0.0203	0.0123	0.0267	1.1	2.03	1.23	2.67	11.82	31.5

derived from *red rose* was considerably higher compared to the other dyes. The analysis also revealed that the extraction of the pigments had dominated the ultrasound technique. However, the variations in the improvement for different petals and leaves may be due to variations in their bonding of coloring material added by cell membranes [32]. The organic components in the extracted dye materials responsible for color and solubility are considered vital variables affecting the improvements of petals, leaves, and composites [71, 72, 73, 74]. In summary, we conclude that the improvement increased by 15–33% in the ethanol-based ultrasonic extraction compared to the water-based magnetic stirring process.

3.5. Aging effects

As dyes degrade with time and temperature, the dyes' aging effect with 60 days interval in an oxygen-rich environment at room temperature and 60 °C has been shown in Figure 9 for (the water solvent). At high pigment concentrations, a strong absorbance peak was observed in the visible region of the spectrum. In *Portulaca grandiflora*, absorption peaks at 252 nm and 312 nm indicated the absorption of flavonoids pigments from 220-380 nm [75]. In contrast, after 60 days at room temperature, these peaks were lost due to the heat sensitivity [76]. It may be occurred due to the chemical degradation through hydrolysis or oxidative reactions, which cuts off different bonds and formation of smaller molecules among water and dyes [77]. As extracted dyes, the absorption peak at 539 nm becomes larger and sharper at room temperature with two additional peaks at 740 nm and 840 nm. However, at 60 °C temperature, all these peaks were disappeared. The two absorption peaks seen in *Rosa ards rover* and *Celosia argentea ver. Cristia* dye (at 362 nm, and 280 nm) were shifted to 983 nm after 60 days both for 25 °C and 60 °C. In contrast to the visible region, *Pereskia bleo* dye displayed several peaks at 452 nm, 478 nm, and 545 nm indicating the occurrence of violaxanthol and phycoerythrins [56]. In comparison, a shift to a flavonoid region at 267 nm was appeared [78].

At 25 °C, only the peak seen at 267 nm sustains while all other visible areas have died out at 60 °C. In the case of *Alternanthera ficoidea* dye, two extremes were detected for the as extracted pigments at 265 nm, and 337 nm, while new peaks were visualized at 674 nm, and 747 nm after the aging at room temperature. The 60 days aging at 60 °C indicated a hypsochromic shift of the peak from 674 nm (25 °C) to 671 nm. During the aging, all dyes have shown an individual rise at 983 nm at room temperature and 60 °C. All five extracted dyes have demonstrated blue shifts due to natural aging, exposure to solar irradiation, and degradation of the pigments [79]. From the above discussions, we signposted that as extracted dyes exhibited more significant activity than that of 60 days interval (both 25 °C and 60 °C temperature) under incident light (see Figure 9 (a)–(e)).

From Table 6, it can be easily claimed that the direct and indirect bandgaps of natural dyes after 60 days are continuously increasing at room temperature. Still at 60 °C, the bandgaps were significantly decreased except for *portulaca grandiflora* pigment. The aging effect on the transmittance spectra of five different natural dyes at room temperature and 60 °C in a time interval 60 of days has been given in Figure 10. Compared to Figure 7 (as extracted transmittance spectra), there is no fundamental difference between as extracted and 60 days aging at 25 °C whereas 60 days aging at 60 °C has confirmed no residual dyes' transmittance properties at the visible regions. The refractive indices of the water-based extracted natural dyes have been tabulated after the 60 days aging at room temperature and 60 °C, and the results have been summarized in Table 7. After 60 days, the dyes aging at 60 °C have shown a higher refractive index than the extracted and room temperature aged pigments. This predicted the optical density of the samples has significantly increased due to the aging. Since the refractive index value increases after aging at 60 °C, it indicated the increasing optical density and decreasing the speed of light into these materials. The experiment recorded refractive indices of these materials provided by other

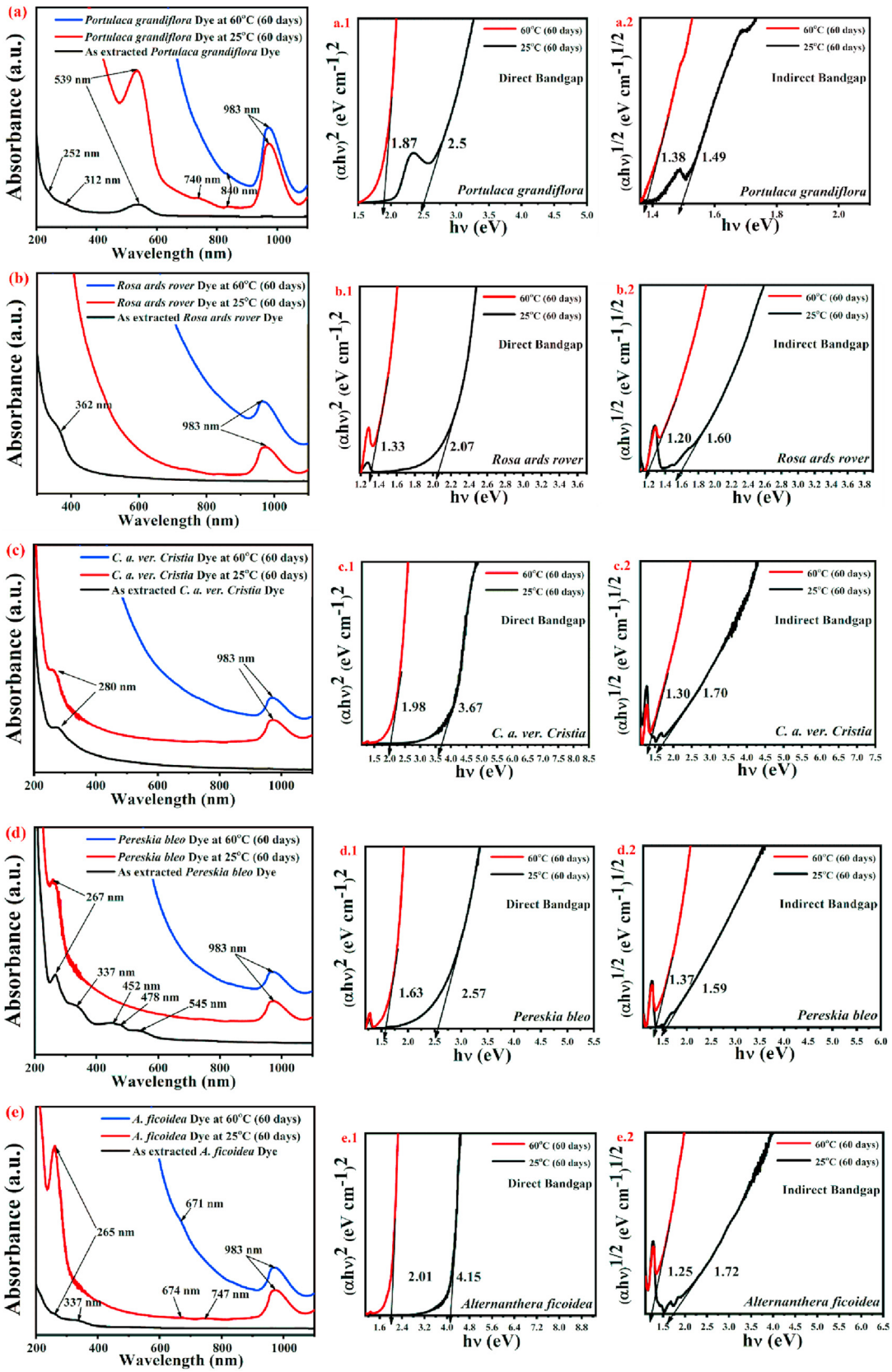

Figure 9. Optical absorption spectra of as extracted, at room temperature (25 °C) and 60 °C temperature after 60 days for (a) *portulaca grandiflora* (b) *rosa ards rovar* (c) *celosia argentea ver. cristia* (d) *pereskia belo* and (e) *alternanthera flcoidea*, where (a.1-e.1) and (a.2-e.2) indicates the plots of $(\alpha h\nu)^2$ versus (hν) (direct bandgap) and $(\alpha h\nu)^{1/2}$ versus (hν) (indirect bandgap) ageing effect of five natural dyes respectively at 25 °C (black curve) and 60 °C (red curve) using Tauc relations.

Table 6. Band gap for natural dyes at room temperature (25 °C) and 60 °C temperature with 60 days interval and comparison with as extracted dyes.

Dye solution	Direct bandgap (eV)			Indirect bandgap (eV)		
	As extracted dyes	After 60 days		As extracted dyes	After 60 days	
		At 25 °C	At 60 °C.		At 25 °C	At 60 °C
Portulaca grandiflora	1.84	2.5	1.87	1.54	1.49	1.38
Rosa ards rover	1.77	2.07	1.33	1.59	1.60	1.20
Celosia argentea ver. Cristia	2.32	3.67	1.98	1.67	1.70	1.30
Pereskia bleo	1.87	2.57	1.63	1.56	1.59	1.37
Alternanthera ficoidea	2.42	4.15	2.01	1.71	1.72	1.25

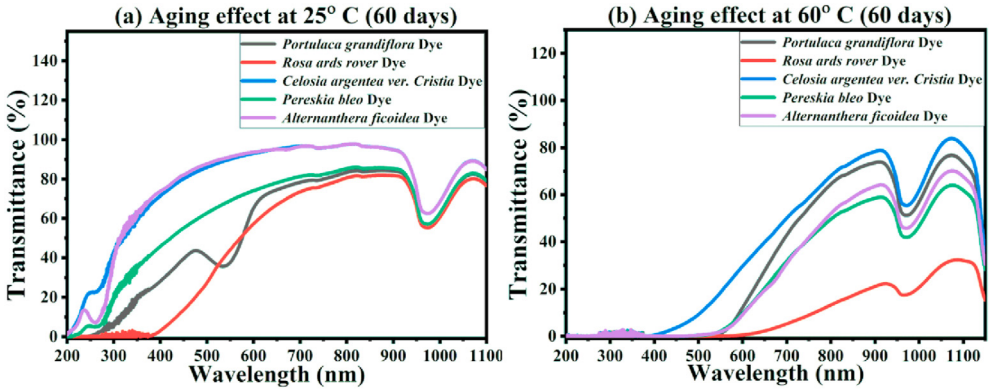

Figure 10. Transmittance spectra of aging effect for five aged (60 days) dye solutions at (a) 25 °C and (b) 60 °C as a function of wavelength (nm).

researchers, nicely validating our estimations [80, 81]. Ollis *et al.* [82] suggested a relationship between the rate of degradation (D) and intensity of incident light (I) on the surface of a material through the following Eqs. (6) and (7),

$$D \propto I \ (at\ low\ light) \tag{6}$$

$$D \propto \sqrt{I} \ (at\ intermediate\ light) \tag{7}$$

Here D is considered to be independent for high incident light. The refractive index has a proportional relationship with dye degradation within a specific limit [83]. The refractive index of the aged dye increases under 60 °C temperature due to the more incident light, *i.e.*, the dye's higher degradation. Again, at 25 °C, the refractive index is very closely compared to extracted dyes. The degradation is also less due to the incident of a lower amount of lights onto the pigments. Further aging effect on the natural dyes have been carried out *via* FTIR spectroscopic studies. Figure 11 reported that the FTIR spectra of five dye samples exhibited substantial degradation (compared to the FTIR data provided in Figure 4) as they have been exposed to the environment (both at room temperature and 60 °C). Significant changes in the FTIR peaks were transpired when aged for 60 days at 60 °C. The vibrational patterns suggested certain photodegradation due to the exposure at oxygen. The FTIR vibrational modes (see Figure 11) have demonstrated variations (compared to Figure 4(a)) in the size and strength at 1722 cm^{-1} (C= O) to 1049 cm^{-1} (C–O) bands and thereby indicating the formation of additional hydrogen bonds for both Figure 11(a) and (b) [84, 85]. Besides, there seemed to be a rising trend of conjugated $–CH_3$, $–CH_2$, C–O functional groups for *Portulaca grandiflora, Rosa ards rover, and Alternanthera ficoidea* (Figure 11(a) at 25 °C) through the bands at 1689 cm^{-1} and 1611 cm^{-1}. It has also been found that molecules split at C–O bond (band amplitude: 1049 cm^{-1}), $–CH_3$ (1311 cm^{-1}), and $–CH_2$ (1400 cm^{-1}) for *Portulaca grandiflora, Rosa ards rover, and Pereskia bleo* at 60 °C after 60 days of aging. Thus, it is appropriate to conclude that C=O groups have been formed simultaneously as the bands' signal increased at 1603 cm-1 and 1250 cm^{-1}. The two giant peaks associated with the surface-adsorbed H_2O, and –OH group at 3500 cm^{-1} (at 25 °C and 60 °C) have been found after 60 days interval [86, 87]. The –OH group performs a significant role (by the stability) in the process of degradation with photogenerated holes *via* light effect, as seen in earlier literature [88]. In the oxygen-rich environment, all dyes' functional groups for both aged temperatures mostly lost their patterns at 1750 cm^{-1} to 1689 cm^{-1}.

Table 7. Calculated refractive index for natural dyes of water solvent at room temperature (25 °C) and 60 °C temperature after 60 days and comparison with as extracted dyes.

Dye solution	Refractive index for water solvent		
	As extracted dyes	After 60 days	
		At 25 °C	At 60 °C.
Portulaca grandiflora	1.5	1.51	9.46
Rosa ards rover	1.55	1.53	10.86
Celosia argentea ver. Cristia	1.51	1.51	6.49
Pereskia bleo	1.51	1.51	8.52
Alternanthera ficoidea	1.51	1.51	8.18

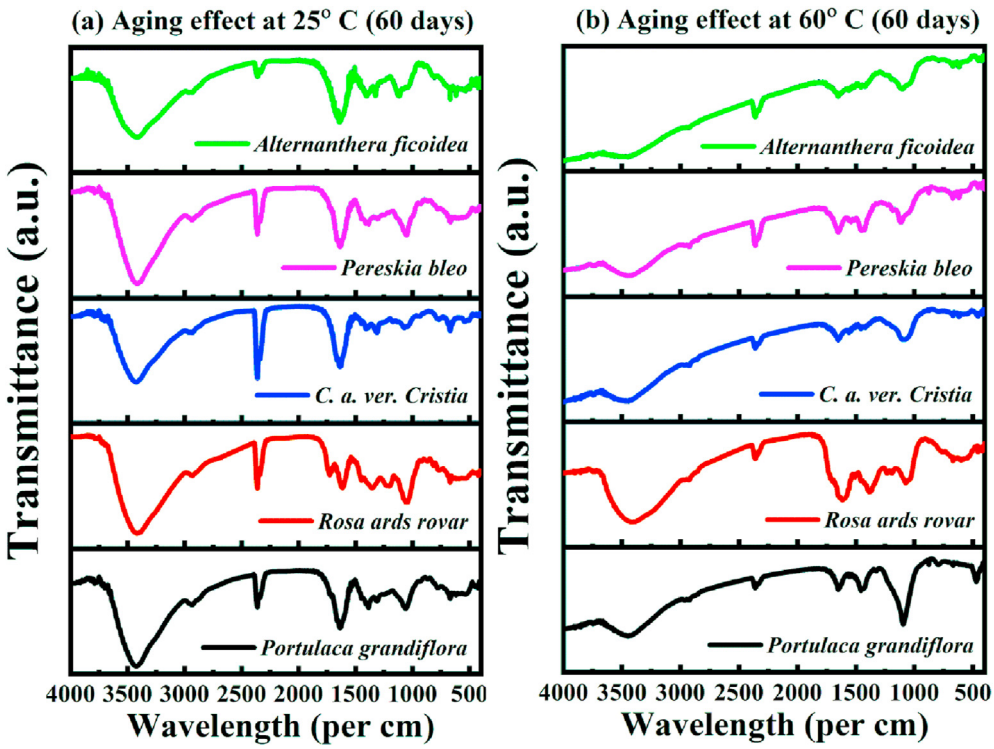

Figure 11. Ageing effect (60 days) Fourier transform infrared (FTIR) spectroscopy of five natural dyes at (a) 25 and (b) 60 °C as a function of wavelength (per cm).

4. Conclusions

This study has exhibited that, *Portulaca grandiflora* (Time Flower), *Rosa ards rovar* (Red Rose), *Celosia argentea var. cristia* (Plumed Cockscomb), *Pereskia bleo* (Desert Rose), and *Alternanthera ficoidea* (Border Plant) dyes can be separated as potential resources using low cost methods. The ultrasound-assisted ethanol-based extraction showed a better improvement from 15% to 33%. The direct bandgap increased from 2.05 eV to 2.32 eV, and the indirect bandgap from 1.77 eV to 2.07 eV, whereas Urbach energy was increased from 3 meV to 14 meV. If the optimum type of wavelength is used, it will provide ideal dyeing conditions for the natural dyes, such as chlorophyll *a*, α carotene, β carotene, Luteol, and phycoerythrin. The solvent's effect on natural dye extraction was identified together with different functional groups from the FTIR results. The aging effects on water-based extracted dyes showed that the direct and indirect bandgaps at room temperature increases from 2.07 eV to 4.15 eV, and from 1.59 eV to 1.72 eV, respectively. However, at 60 °C, the bandgaps were decreased compared to that of the room temperature extracted dyes. Under the aging conditions, the refractive index values remained nearly the same at room temperature, while at 60 °C temperature, it exhibited much higher values (from 6.49 to 10.86). The aging effects of the organic dyes in an oxygen-rich environment significantly helped to apprehend the actual effluent of solar cell applications and photocatalytic analysis. This study will play a substantial role in bringing about a new understanding of the optical behaviors and aging effects of the organic dyes and opening up new opportunities to make better artificial dyes for real-life applications.

Declarations

Author contribution statement

S M Amir-Al Zumahi: Conceived and designed the experiments; Performed the experiments; Analyzed and interpreted the data; Contributed reagents, materials, analysis tools or data; Wrote the paper.

Nourin Arobi, Hatem Taha, Md Kamal Hossain, Humayun Kabir, Rummana Matin, M S Bashar: Performed the experiments; Analyzed and interpreted the data; Contributed reagents, materials, analysis tools or data; Wrote the paper.

Farid Ahmed, Md Abul Hossain, M Mahbubur Rahman: Conceived and designed the experiments; Analyzed and interpreted the data; Contributed reagents, materials, analysis tools or data; Wrote the paper.

Funding statement

This work was supported by the Ministry of Science and Technology, Government of the People's Republic of Bangladesh.

Competing interest statement

The authors declare no conflict of interest.

Additional information

No additional information is available for this paper.

References

[1] M. Hussaan, N. Iqbal, S. Adeel, M. Azeem, M.T. Javed, A. Raza, Microwave-assisted enhancement of milkweed (Calotropis procera L.) leaves as an eco-friendly source of natural colorants for textile, Environ. Sci. Pollut. Control Ser. 24 (5) (2017) 5089–5094.
[2] Joseph Sarkis, Laura M. Meade, Talluri Srinivas, E-logistics and the natural environment, Supply Chain Manag.: Int. J. 9 (4) (2004) 303–312.
[3] M.H. Fulekar, Bioremediation Technology for hazardous wastes-recent advances, in: Bioremediation Technology, Springer, Dordrecht, 2010, pp. 135–166.
[4] Mohammad Shahid, Faqeer Mohammad, Recent advancements in natural dye applications: a review, J. Clean. Prod. 53 (2013) 310–331.
[5] F. Pozzi, S. Zaleski, F. Casadio, M. Leona, J.R. Lombardi, Van Duyne, Surface-enhanced Raman spectroscopy: using nanoparticles to detect trace amounts of colorants in works of art, in: Nanoscience and Cultural Heritage, Atlantis Press, Paris, 2016, pp. 161–204.
[6] José Alberto Caram, M.J. Banera, JF Martínez Suárez, Maria Virginia Mirifico, Electrochemical behaviour of Anthraquinone dyes in non-aqueous solvent solution:

Part I. Medium effect on the electrochemical behavior, Electrochim. Acta 249 (2017) 431–445.
[7] C.I. Pearce, J.R. Lloyd, J.T. Guthrie, The removal of colour from textile wastewater using whole bacterial cells: a review, Dyes Pigments 58 (3) (2003) 179–196.
[8] G. McMullan, C. Meehan, A. Conneely, N. Kirby, T. Robinson, P. Nigam, I. Banat, R. Marchant, W. Smyth, Microbial decolourisation and degradation of textile dyes, Appl. Microbiol. Biotechnol. 56 (1-2) (2001) 81–87.
[9] G. Nagendrappa, Sir William Henry Perkin: the man and his 'mauve', Resonance 15 (9) (2010) 779–793.
[10] Özlenen Erdem Ismal, Boyarmadde Endüstrisinin Öncüsü: bir bilim adamı ve entelektüel olarak Sir WILLIAM HENRY PERKIN, Yedi 6 (2011) 23–30.
[11] Lintao Yu, Xiangge Zhou, Di Wu, Haifeng Xiang, Synthesis of phenazines by Cu-catalyzed homocoupling of 2-halogen anilines in water, J. Organomet. Chem. 705 (2012) 75–78.
[12] Petra Amchova, Hana Kotolova, Jana Ruda-Kucerova, Health safety issues of synthetic food colorants, Regul. Toxicol. Pharmacol. 73 (3) (2015) 914–922.
[13] Torgils Fossen, Luis Cabrita, Oyvind M. Andersen, Colour and stability of pure anthocyanins influenced by pH including the alkaline region, Food Chem. 63 (4) (1998) 435–440.
[14] Jean-Baptiste Tarkwa, Nihal Oturan, Elie Acayanka, Samuel Laminsi, A. Mehmet, Oturan, Photo-Fenton oxidation of Orange G azo dye: process optimization and mineralization mechanism, Environ. Chem. Lett. 17 (1) (2019) 473–479.
[15] Shrikant S. Thakare, Mavila C. Sreenath, Subramaniyan Chitrambalam, Isaac H. Joe, Nagaiyan Sekar, Non-linear optical study of BODIPY-benzimidazole conjugate by solvatochromic, Z-scan and theoretical methods, Opt. Mater. 64 (2017) 453–460.
[16] P Narayana Prasad, David John Williams, Introduction to Nonlinear Optical Effects in Molecules and Polymers, Wiley, New York, 1990.
[17] B. Ballantyne, Local and systemic ophthalmic pharmacology and toxicology of organophosphate and carbamate anticholinesterases, in: Toxicology of Organophosphate & Carbamate Compounds, Academic Press, 2006, pp. 423–445.
[18] Flavia R. Abe, Jacqueline N. Mendonça, Luiz AB. Moraes, Gisele AR. de Oliveira, Carlos Gravato, Amadeu MVM. Soares, Danielle P. de Oliveira, Toxicological and behavioral responses as a tool to assess the effects of natural and synthetic dyes on zebrafish early life, Chemosphere 178 (2017) 282–290.
[19] Nadia Morin-Crini, Eric Lichtfouse, Giangiacomo Torri, Grégorio Crini, Applications of chitosan in food, pharmaceuticals, medicine, cosmetics, agriculture, textiles, pulp and paper, biotechnology, and environmental chemistry, Environ. Chem. Lett. 17 (2019) 1667–1692.
[20] Piero Savarino, Viscardi Guido, Pierluigi Quagliotto, Enzo Montoneri, Ermanno Barni, Reactivity and effects of cyclodextrins in textile dyeing, Dyes Pigments 42 (2) (1999) 143–147.
[21] Xizhe Fu, Tarun Belwal, Giancarlo Cravotto, Zisheng Luo, Sono-physical and sono-chemical effects of ultrasound: primary applications in extraction and freezing operations and influence on food components, Ultrason. Sonochem. 60 (2020) 104726.
[22] Asmaa Soheil Najm, Norasikin A. Ludin, Mahir Faris Abdullah, Munirah A. Almessiere, Naser M. Ahmed, Mahmoud AM. Al-Alwani, Areca catechu extracted natural new sensitizer for dye-sensitized solar cell: performance evaluation, J. Mater. Sci. Mater. Electron. 31 (4) (2020) 3564–3575.
[23] Madeleine Jönsson, Leila Allahgholi, Roya RR. Sardari, O. Guðmundur, Hreggviðsson, Eva Nordberg Karlsson, Extraction and modification of macroalgal polysaccharides for current and next-generation applications, Molecules 25 (4) (2020) 930.
[24] Mohaddeseh Afshari, Mohammad Dinari, Synthesis of new imine-linked covalent organic framework as high efficient absorbent and monitoring the removal of direct fast scarlet 4BS textile dye based on mobile phone colorimetric platform, J. Hazard Mater. 385 (2020) 121514.
[25] Luqman Jameel Rather, Qi Zhou, Asghar Ali, Qazi Mohd Rizwanul Haque, Qing Li, Valorization of natural dyes extracted from Mugwort leaves (Folium artemisiae argyi) for wool fabric dyeing: optimization of extraction and dyeing processes with simultaneous coloration and biofunctionalization, ACS Sustain. Chem. Eng. 8 (7) (2020) 2822–2834.
[26] Irena Žuntar, Predrag Putnik, Danijela Bursać Kovačević, Marinela Nutrizio, Šupljika Filip, Andreja Poljanec, Igor Dubrović, Francisco J. Barba, Anet Režek Jambrak, Phenolic and antioxidant analysis of olive leaves extracts (olea europaea L.) obtained by high voltage electrical discharges (HVED), Foods 8 (7) (2019) 248.
[27] Monica Gallo, Rosalia Ferracane, Giulia Graziani, Alberto Ritieni, Vincenzo Fogliano, Microwave assisted extraction of phenolic compounds from four different spices, Molecules 15 (9) (2010) 6365–6374.
[28] Shekhar U. Kadam, Colm P. O'Donnell, Dilip K. Rai, Mohammad B. Hossain, Catherine M. Burgess, Des Walsh, Brijesh K. Tiwari, Laminarin from Irish brown seaweeds Ascophyllum nodosum and Laminaria hyperborea: ultrasound assisted extraction, characterization and bioactivity, Mar. Drugs 13 (7) (2015) 4270–4280.
[29] Liazid Ali, Gerardo F. Barbero, Latifa Azaroual, Miguel Palma, Carmelo G. Barroso, Stability of anthocyanins from red grape skins under pressurized liquid extraction and ultrasound-assisted extraction conditions, Molecules 19 (12) (2014) 21034–21043.
[30] Bimal Chitrakar, Min Zhang, Bhesh Bhandari, Edible flowers with the common name "marigold": their therapeutic values and processing, Trends Food Sci. Technol. 89 (2019) 76–87.
[31] Mohd Shabbir, Luqman Jameel Rather, Faqeer Mohammad, Economically viable UV-protective and antioxidant finishing of wool fabric dyed with Tagetes erecta flower extract: valorization of marigold, Ind. Crop. Prod. 119 (2018) 277–282.
[32] Venkatasubramanian Sivakumar, J. Vijaeeswarri, J. Lakshmi Anna, Effective natural dye extraction from different plant materials using ultrasound, Ind. Crop. Prod. 33 (1) (2011) 116–122.
[33] Shahid-ul-Islam, Luqman Jameel Rather, Mohd Shabbir, Javed Sheikh, Mohd Nadeem Bukhari, Mohd Ali Khan, Faqeer Mohammad, Exploiting the potential of polyphenolic biomordants in environmentally friendly coloration of wool with natural dye from Butea monosperma flower extract, J. Nat. Fibers 16 (4) (2019) 512–523.
[34] Ho Chang, Yu-Jen Lo, Pomegranate leaves and mulberry fruit as natural sensitizers for dye-sensitized solar cells, Sol. Energy 84 (10) (2010) 1833–1837.
[35] Jeevan K. Prasain, Stephen Barnes, Novel Diarylheptanoids and metabolism and bioavailablity of curcumin, Stud. Nat. Prod. Chem. 47 (2016) 201–214.
[36] Chunxia Wang, Changhai Xu, Anli Tian, Shaohai Fu, Chaoxia Wang, Extraction of natural dyes from Alpinia blepharocalyx K. Schum. for dyeing of silk fabric, Color. Technol. 129 (1) (2013) 32–38.
[37] Matteo Bordiga, Fabiano Travaglia, Monica Locatelli, Valorisation of grape pomace: an approach that is increasingly reaching its maturity–a review, Int. J. Food Sci. Technol. 54 (4) (2019) 933–942.
[38] Mohd Yusuf, Mohammad Shahid, Mohd Ibrahim Khan, Shafat Ahmad Khan, Mohd Ali Khan, Faqeer Mohammad, Dyeing studies with henna and madder: a research on effect of tin (II) chloride mordant, J. Saudi Chem. Soc. 19 (1) (2015) 64–72.
[39] Md Motiar R. Khan, Bijendra Sahoo, Ashok K. Mukherjee, Animesh Naskar, Biosorption of acid yellow-99 using mango (Mangifera indica) leaf powder, an economic agricultural waste, SN Appl. Sci. 1 (11) (2019) 1493.
[40] Varinder Kaur, Manish Kumar, Paramjeet Kaur, Sandeep Kaur, Satwinderjeet Kaur, Inhibitory activities of butanol fraction from Butea monosperma (Lam.) Taub. bark against free radicals, genotoxins and cancer cells, Chem. Biodivers. 14 (6) (2017), e1600484.
[41] Feriel Bouatay, Noureddine Baaka, Adeel Shahid, Mohamed Farouk Mhenni, A novel natural source Vicia faba L. membranes as colourant: development and optimisation of the extraction process using response surface methodology (RSM), Nat. Prod. Res. 33 (1) (2019) 59–65.
[42] Katrin Gossen, Jan Lukas Storck, Andrea Ehrmann, Influence of solvents on Aloe vera gel performance in dye-sensitized solar cells, Optik 180 (2019) 615–618.
[43] Suraweera Arachchilage Tharindu Lakshan, Nileththi Yasendra Jayanath, Walimuni Prabhashini Kaushalya Mendis Abeysekera, Walimuni Kanchana Subhashini Mendis Abeysekera, A commercial potential blue pea (clitoria ternatea L.) flower extract incorporated beverage having functional properties, Evid. base Compl. Alternative Med. (2019) 13.
[44] Bin Huang, Hao Rong, Youju Ye, Zhouxian Ni, Meng Xu, Wangxiang Zhang, Li-an Xu, Transcriptomic analysis of flower color variation in the ornamental crabapple (Malus spp.) half-sib family through Illumina and PacBio Sequel sequencing, Plant Physiol. Biochem. 149 (2020) 27–35.
[45] Polturak Guy, Asaph Aharoni, "La Vie En Rose": biosynthesis, sources, and applications of betalain pigments, Mol. Plant 11 (1) (2018) 7–22.
[46] Yuhan Tang, Ziwen Fang, Mi Liu, Daqiu Zhao, Jun Tao, Color characteristics, pigment accumulation and biosynthetic analyses of leaf color variation in herbaceous peony (Paeonia lactiflora Pall.), 3 Biotech 10 (2) (2020) 76.
[47] Regina Cortez, Diego A. Luna-Vital, Daniel Margulis, Elvira Gonzalez de Mejia, Natural pigments: stabilization methods of anthocyanins for food applications, Compr. Rev. Food Sci. Food Saf. 16 (1) (2017) 180–198.
[48] Hca Van Beek, M. Pieter, Heertjes, Fading by light of organic dyes on textiles and other materials, Stud. Conserv. 11 (3) (1966) 123–132.
[49] Patrick Dietemann, Moritz Kälin, Stefan Zumbühl, Richard Knochenmuss, Stefan Wülfert, Renato Zenobi, A mass spectrometry and electron paramagnetic resonance study of photochemical and thermal aging of triterpenoid varnishes, Anal. Chem. 73 (9) (2001) 2087–2096.
[50] J.S. Arne, A.J. Jacobs, Richard Newman, The influence of oxygen on the fading of organic colorants, J. Am. Inst. Conserv. 18 (2) (1979) 108–117.
[51] John W. Weigl, Robert Livingston, Infrared spectra of chlorophyll and related compounds, J. Am. Chem. Soc. 75 (9) (1953) 2173–2176.
[52] A.S. Holt, E.E. Jacobs, Infra-red absorption spectra of chlorophylls and derivatives, Plant physiology 30 (6) (1955) 553.
[53] R. Nayak, S. Houshyar, A. Khandual, R. Padhye, S. Fergusson, Identification of natural textile fibres, in: Handbook of natural fibres, 1, Woodhead Publishing, 2020, pp. 503–534.
[54] Wei Wang, Jinggang Wang, Yunliang Zhao, Haoyu Bai, Muyang Huang, Tingting Zhang, Shaoxian Song, High-performance two-dimensional montmorillonite supported-poly (acrylamide-co-acrylic acid) hydrogel for dye removal, Environ. Pollut. 257 (2020) 113574.
[55] G.R.A. Kumara, S. Kaneko, M. Okuya, B. Onwona-Agyeman, A. Konno, K. Tennakone, Shiso leaf pigments for dye-sensitized solid-state solar cell, Sol. Energy Mater. Sol. Cell. 90 (9) (2006) 1220–1226.
[56] Anandita, Structure, Chemical Composition and Development of Chloroplast (n.d.); Retrieved from Biology Discussion: http://www.biologydiscussion.com/chloroplasts/structure-chemical-composition-and-development-of-chloroplast/3991.
[57] Eka Cahya Prima, Novianto Nur Hidayat, Brian Yuliarto, Hermawan Kresno Dipojono, A combined spectroscopic and TDDFT study of natural dyes extracted from fruit peels of Citrus reticulata and Musa acuminata for dye-sensitized solar cells, Spectrochim. Acta Mol. Biomol. Spectrosc. 171 (2017) 112–125.
[58] A. Amri, K. Hasan, H. Taha, M.M. Rahman, S. Herman, E. Awaltanova, H. Kabir, C.-Y. Yin, K. Ibrahim, S. Bahri, Surface structural features and optical analysis of nanostructured Cu-oxide thin film coatings coated via the sol-gel dip coating method, Ceram. Int. 45 (10) (2019) 12888–12894.

[59] K. Ibrahim, H. Taha, M.M. Rahman, H. Kabir, Z.-T. Jiang, Solar selective performance of metal nitride/oxynitride based magnetron sputtered thin film coatings: a comprehensive review, J. Optic. 20 (3) (2018), 033001.
[60] H. Kabir, R. Nasrin, M.M. Rahman, A. Bhuiyan, Heat treatment effect on the structural, morphological, and optical properties of plasma polymerized furan-2-carbaldehyde thin films, Res. Phys. 16 (2020) 103014.
[61] A. Hafdallah, F. Yanineb, M.S. Aida, N. Attaf, In doped ZnO thin films, J. Alloys Compd. 509 (26) (2011) 7267–7270.
[62] Sema Ebrahimi, Benyamin Yarmand, Solvothermal growth of aligned SnxZn1-xS thin films for tunable and highly response self-powered UV detectors, J. Alloys Compd. 827 (2020) 154246.
[63] Leiping Duan, Haimang Yi, Yu Zhang, Faiazul Haque, Cheng Xu, Ashraf Uddin, Comparative study of light-and thermal-induced degradation for both fullerene and non-fullerene-based organic solar cells, Sustain. Energy Fuel. 3 (3) (2019) 723–735.
[64] Essam R. Shaaban, Ishu Kansal, S.H. Mohamed, Joés MF. Ferreira, Microstructural parameters and optical constants of ZnTe thin films with various thicknesses, Phys. B Condens. Matter 404 (20) (2009) 3571–3576.
[65] Matthew S. Bigelow, Nick N. Lepeshkin, Robert W. Boyd, Observation of ultraslow light propagation in a ruby crystal at room temperature, Phys. Rev. Lett. 90 (11) (2003) 113903.
[66] Miłosz Pawlicki, Hazel A. Collins, Robert G. Denning, Harry L. Anderson, Two-photon absorption and the design of two-photon dyes, Angew. Chem. Int. Ed. 48 (18) (2009) 3244–3266.
[67] D.A. Duarte, Marcos Massi, A.S. da Silva Sobrinho, Development of dye-sensitized solar cells with sputtered N-doped thin films: from modeling the growth mechanism of the films to fabrication of the solar cells, Int. J. Photoenergy (2014) 13.
[68] K.B. Kahen, Jean-Pierre Leburton, Optical constants of GaAs-$Al_xGa_{1-x}As$ superlattices and multiple quantum wells, Phys. Rev. B 33 (8) (1986) 5465.
[69] M.A. Rauf, John P. Graham, Saeed B. Bukallah, Mariam AS. Al-Saedi, Solvatochromic behavior on the absorption and fluorescence spectra of Rose Bengal dye in various solvents, Spectrochim. Acta Mol. Biomol. Spectrosc. 72 (1) (2009) 133–137.
[70] Venkatasubramanian Sivakumar, J. Lakshmi Anna, J. Vijayeeswarri, G. Swaminathan, Ultrasound assisted enhancement in natural dye extraction from beetroot for industrial applications and natural dyeing of leather, Ultrason. Sonochem. 16 (6) (2009) 782–789.
[71] Reife Abraham, Dyes, Environmental Chemistry, Kirk-Othmer Encyclopedia of Chemical Technology, 2000.
[72] S. Jeyaram, T. Geethakrishnan, Linear and nonlinear optical properties of chlorophyll-a extracted from Andrographis paniculata leaves, Optic Laser. Technol. 116 (2019) 31–36.
[73] V. Selvaraj, K.P. Jayanthi, K. Arunkumar, S. Jeyaram, T. Geethakrishnan, M. Alagar, Synthesis and characterization of GO doped bio-resource based composites for NLO and multifaceted applications, J. Polym. Res. 27 (3) (2020) 1–16.
[74] S. Jeyaram, T. Geethakrishnan, Solvent dependent linear and nonlinear optical characteristics of acid blue 3 dye, J. Fluoresc. (2020) 1–9.
[75] S. Hosseini Sarghein, J. Carapetian, J. Khara, Effects of UV-radiation on photosynthetic pigments and UV absorbing compounds in Capsicum longum (L.), Int. J. Bot. 4 (4) (2008) 486–490.
[76] Xinxin Zhang, Xin Wang, Minglong Wang, Jianguo Cao, Jianbo Xiao, Quanxi Wang, Effects of different pretreatments on flavonoids and antioxidant activity of Dryopteris erythrosora leave, PloS One 14 (1) (2019), e0200174.
[77] Lüttge Ulrich, Physiological Ecology of Tropical Plants, Springer Science & Business Media, 2007.
[78] F. Hollósy, Effects of ultraviolet radiation on plant cells, Micron 33 (2) (2002) 179–197.
[79] Marta Anghelone, Dubravka Jembrih-Simbürger, Manfred Schreiner, Influence of phthalocyanine pigments on the photo-degradation of alkyd artists' paints under different conditions of artificial solar radiation, Polym. Degrad. Stabil. 134 (2016) 157–168.
[80] I.A. McIntyre, M.H. Dunn, Measurement of the temperature dependence of refractive index of dye laser solvents, J. Phys. E Sci. Instrum. 18 (1) (1985) 19.
[81] Ş. Yaltkaya, Ramazan Aydin, Experimental investigation of temperature effect on refractive index of dye laser liquids, Turk. J. Phys. 26 (1) (2001) 41–48.
[82] David F. Ollis, Ezio Pelizzetti, Nick Serpone, Photocatalyzed destruction of water contaminants, Environ. Sci. Technol. 25 (9) (1991) 1522–1529.
[83] Masanobu Yoshida, Katsumi Uchida, Masamichi Kato, Yoshinori Konishi, New diagnosis method of aging degradation for insulating paper in power transformers by measuring the refractive index of cellulose fibers, in: 2012 IEEE International Conference on Condition Monitoring and Diagnosis, 2012, pp. 56–59.
[84] Monika Koperska, Tomasz Łojewski, Joanna Łojewska, Vibrational spectroscopy to study degradation of natural dyes. Assessment of oxygen-free cassette for safe exposition of artefacts, Anal. Bioanal. Chem. 399 (9) (2011) 3271–3283.
[85] M.A. Signore, A. Sytchkova, D. Dimaio, A. Cappello, A. Rizzo, Deposition of silicon nitride thin films by RF magnetron sputtering: a material and growth process study, Opt. Mater. 34 (4) (2012) 632–638.
[86] Tianyou Peng, De Zhao, Haibo Song, Chunhua Yan, Preparation of lanthana-doped titania nanoparticles with anatase mesoporous walls and high photocatalytic activity, J. Mol. Catal. Chem. 238 (1-2) (2005) 119–126.
[87] Jimmy C. Yu, Lizhi Zhang, Zhi Zheng, Jincai Zhao, Synthesis and characterization of phosphated mesoporous titanium dioxide with high photocatalytic activity, Chem. Mater. 15 (11) (2003) 2280–2286.
[88] Zhiying Yan, Wenjuan Gong, Yongjuan Chen, Deliang Duan, Junjie Li, Wei Wang, Jiaqiang Wang, Visible-light degradation of dyes and phenols over mesoporous titania prepared by using anthocyanin from red radish as template, Int. J. Photoenergy (2014) 968298.